

New Measurements of Nucleon Structure Functions from the CCFR/NuTeV Collaboration

A. Bodek,⁷ U. K. Yang,⁷ T. Adams,⁴ A. Alton,⁴ C. G. Arroyo,² S. Avvakumov,⁷ L. de Barbaro,⁵ P. de Barbaro,⁷ A. O. Bazarko,² R. H. Bernstein,³ T. Bolton,⁴ J. Brau,⁶ D. Buchholz,⁵ H. Budd,⁷ L. Bugel,³ J. Conrad,² R. B. Drucker,⁶ B. T. Fleming,² J. A. Formaggio,² R. Frey,⁶ J. Goldman,⁴ M. Goncharov,⁴ D. A. Harris,⁷ R. A. Johnson,¹ J. H. Kim,² B. J. King,² T. Kinnel,⁸ S. Koutsoliotas,² M. J. Lamm,³ W. Marsh,³ D. Mason,⁶ K. S. McFarland,⁷ C. McNulty,² S. R. Mishra,² D. Naples,⁴ P. Nienaber,³ A. Romosan,² W. K. Sakumoto,⁷ H. Schellman,⁵ F. J. Sciulli,² W. G. Seligman,² M. H. Shaevitz,² W. H. Smith,⁸ P. Spentzouris,² E. G. Stern,² M. Vakili,¹ A. Vaitaitis,² V. Wu,¹ J. Yu,³ G. P. Zeller,⁵ and E. D. Zimmerman²
(The CCFR/NuTeV Collaboration)

¹ *Univ. of Cincinnati, Cincinnati, OH 45221*; ² *Columbia University, New York, NY 10027*
³ *Fermilab, Batavia, IL 60510* ⁴ *Kansas State University, Manhattan, KS 66506*
⁵ *Northwestern University, Evanston, IL 60208*; ⁶ *Univ. of Oregon, Eugene, OR 97403*
⁷ *Univ. of Rochester, Rochester, NY 14627*; ⁸ *Univ. of Wisconsin, Madison, WI 53706*
Presented by Arie Bodek

Abstract. We report on the extraction of the structure functions F_2 and $\Delta xF_3 = xF_3^\nu - xF_3^{\bar{\nu}}$ from CCFR ν_μ -Fe and $\bar{\nu}_\mu$ -Fe differential cross sections. The extraction is performed in a physics model independent (PMI) way. This first measurement for ΔxF_3 , which is useful in testing models of heavy charm production, is higher than current theoretical predictions. The F_2 (PMI) values measured in ν_μ and μ scattering are in good agreement with the predictions of Next to Leading Order PDFs (using massive charm production schemes), thus resolving the long-standing discrepancy between the two sets of data.

Deep inelastic lepton-nucleon scattering experiments have been used to determine the quark distributions in the nucleon. However, the quark distributions determined

from muon and neutrino experiments were found to be different at small values of x , because of a disagreement in the extracted structure functions. Here, we report on a measurement of differential cross sections and structure functions from CCFR ν_μ -Fe and $\bar{\nu}_\mu$ -Fe data. We find that the neutrino-muon difference is resolved by extracting the ν_μ structure functions in a physics model independent way.

The sum of ν_μ and $\bar{\nu}_\mu$ differential cross sections for charged current interactions on an isoscalar target is related to the structure functions as follows:

$$F(\epsilon) \equiv \left[\frac{d^2\sigma^\nu}{dx dy} + \frac{d^2\sigma^{\bar{\nu}}}{dx dy} \right] \frac{(1-\epsilon)\pi}{y^2 G_F^2 M E_\nu} = 2xF_1[1 + \epsilon R] + \frac{y(1-y/2)}{1+(1-y)^2} \Delta x F_3.$$

Here G_F is the Fermi weak coupling constant, M is the nucleon mass, E_ν is the incident energy, the scaling variable $y = E_h/E_\nu$ is the fractional energy transferred to the hadronic vertex, E_h is the final state hadronic energy, and $\epsilon \simeq 2(1-y)/(1+(1-y)^2)$ is the polarization of the virtual W boson. The structure function $2xF_1$ is expressed in terms of F_2 by $2xF_1(x, Q^2) = F_2(x, Q^2) \times \frac{1+4M^2x^2/Q^2}{1+R(x, Q^2)}$, where Q^2 is the square of the four-momentum transfer to the nucleon, $x = Q^2/2ME_h$ (the Bjorken scaling variable) is the fractional momentum carried by the struck quark, and $R = \frac{\sigma_L}{\sigma_T}$ is the ratio of the cross-sections of longitudinally- to transversely-polarized W -bosons. The $\Delta x F_3$ term, which in leading order $\simeq 4x(s-c)$, is not present in the μ -scattering case. In addition, in a ν_μ charged current interaction with s (or \bar{c}) quarks, there is a threshold suppression originating from the production of heavy c quarks in the final state. For μ -scattering, there is no suppression for scattering from s quarks, but more suppression when scattering from c quarks since there are two heavy quarks (c and \bar{c}) in the final state.

In previous analyses of ν_μ data, light-flavor universal physics model dependent (PMD) structure functions were extracted by applying a slow rescaling correction to correct for the charm mass suppression in the final state. In addition, the $\Delta x F_3$ term (used as input in the extraction) was calculated from a leading order charm production model. These resulted in a physics model dependent (PMD) structure functions. In the new analysis reported here, slow rescaling corrections are not applied, and $\Delta x F_3$ and F_2 are extracted from two parameter fits to the data. We compare the values of $\Delta x F_3$ to various charm production models. The extracted physics model independent (PMI) values for F_2^ν are then compared with F_2^μ within the framework of NLO models for massive charm production.

The CCFR experiment collected data using the Fermilab Tevatron Quad-Triplet wide-band ν_μ and $\bar{\nu}_\mu$ beam. The raw differential cross sections per nucleon on iron are determined in bins of x , y , and E_ν ($0.01 < x < 0.65$, $0.05 < y < 0.95$, and $30 < E_\nu < 360$ GeV). Figure 1 (a) shows typical differential cross sections at $E_\nu = 150$ GeV. Next, the raw cross sections are corrected for electroweak radiative effects, the W boson propagator, and for the 5.67% non-isoscalar excess of neutrons over protons in iron (only important at high x). Values of $\Delta x F_3$ and F_2 are extracted from the sums of the corrected ν_μ -Fe and $\bar{\nu}_\mu$ -Fe differential cross sections at different energy bins according to Eq. (1). It is challenging to fit $\Delta x F_3$, R , and $2xF_1$ using the y distribution at a given x and Q^2 because of the strong correlation between

the ΔxF_3 and R terms, unless the full range of y is covered by the data. Covering this range (especially the high y region) is hard because of the low acceptance. Therefore, we restrict the analysis to two parameter fits. Our strategy is to fit ΔxF_3 and $2xF_1$ (or equivalently F_2) for $x < 0.1$ where the ΔxF_3 contribution is relatively large, while constraining R using the $R_{world}^{\mu/e}$ QCD inspired empirical fit to all available R from electron- and μ -scattering data. The $R_{world}^{\mu/e}$ fit is also in good agreement with NMC R^μ data at low x , and with the most recent NNLO QCD calculations (including target mass effects) of R by Bodek and Yang

For $x < 0.1$, R in neutrino scattering is expected to be somewhat larger than R for muon scattering because of the production of massive charm quarks in the final state. A correction for this difference is applied to $R_{world}^{\mu/e}$ using a leading order slow rescaling model to obtain an effective R for neutrino scattering, R_{eff}^ν . The difference between $R_{world}^{\mu/e}$ and R_{eff}^ν is used as a systematic error. Because of the positive correlation between R and ΔxF_3 , the extracted values of F_2 are rather insensitive to the input R . If a large input R is used, a larger value of xF_3 is extracted from the y distribution, thus yielding the same value of F_2 . In contrast, the extracted values of ΔxF_3 are sensitive to the assumed value of R , which is reflected in a larger systematic error. The values of ΔxF_3 are sensitive to the energy dependence of the neutrino flux ($\sim y$ dependence), but are insensitive to the absolute normalization. The uncertainty on the flux shape is estimated by using the constraint that F_2 and xF_3 should be flat over y (or E_ν) for each x and Q^2 bin.

Because of the limited statistics, we use large bins in Q^2 in the extraction of ΔxF_3 with bin centering corrections from the NLO Thorne & Roberts Variable Flavor Scheme (TR-VFS) calculation with the MRST PDFs. Figure 1 (b) shows the extracted values of ΔxF_3 as a function of x , including both statistical and systematic errors, compared to various theoretical methods for modeling heavy charm productions within a QCD framework. The three-flavor Fixed Flavor Scheme (FFS) assumes that there is no intrinsic charm in the nucleon, and all scattering from c quarks occurs via the gluon-fusion diagram. The concept behind the Variable Flavor Scheme (VFS) proposed by ACOT is that at low scale, μ , one uses the three-flavor FFS scheme, and above some scale, one changes to a four-flavor calculation and an intrinsic charm sea (which is evolved from zero) is introduced. The concept in the RT-VFS scheme is that it starts with the three-flavor FFS scheme at a low scale, becomes the four-flavor VFS scheme at high scale, and interpolates smoothly between the two regions. Shown are the predictions from the TR-VFS scheme (as corrected after DIS-2000 and implemented with MRST PDFs), with their suggested scale $\mu = Q$, and the predictions of the other two NLO calculations, ACOT-VFS (implemented with CTEQ4HQ and the recent ACOT suggested scale $\mu = m_c$ for $Q < m_c$, and $\mu^2 = m_c^2 + cQ^2(1 - m_c^2/Q^2)^n$ for $Q < m_c$ with $c = 0.5$ and $n = 2$), and the FFS (implemented with the GRV94 PDFs and GRV94 recommended scale $\mu = 2m_c$). Also shown are the predictions from $\Delta xF_3 \simeq 4Ks(x, Q^2)$ from a leading order model (LO(CCFR)) Buras-Gaemers type fit to the CCFR dimuon data (here

K is a slow rescaling correction). Figure 1 (b) (right) also shows the sensitivity to the choice of scale. The data do not favor the ACOT-VFS(CTEQ4HQ) predictions if implemented with an earlier suggested scale of $\mu = 2Pt_{max}$. With reasonable choices of scale, all the theoretical models yield similar results. However, at low Q^2 our ΔxF_3 data are higher than all the theoretical models. The difference between data and theory may be due to an underestimate of the strange sea (or gluon distribution) at low Q^2 , or from missing NNLO terms.

As discussed above, values of F_2 (PMI) for $x < 0.1$ are extracted from two parameter fits to the y distributions. In the $x > 0.1$ region, the contribution from ΔxF_3 is small and the extracted values of F_2 are insensitive to ΔxF_3 . Therefore, we extract values of F_2 with an input value of R and with ΔxF_3 constrained to the TR-VFS(MRST) predictions. As in the case of the two parameter fits for $x < 0.1$, no corrections for slow rescaling are applied. Fig. 2 (a) shows our F_2 (PMI) measurements divided by the predictions from the TR-VFS(MRST) theory. Also shown are F_2^{μ} and F_2^e from the NMC divided by the theory predictions. In the calculation of the QCD TR-VFS(MRST) predictions, we have also included corrections for nuclear effects, target mass and higher twist corrections at low values of Q^2 . As seen in Fig. 2, both the CCFR and NMC structure functions are in good agreement with the TR-VFS(MRST) predictions, and therefore in good agreement with each other. A comparison using the ACOT-VFS(CTEQ4HQ) predictions yields similar results.

In the previous analysis of the CCFR data, the extracted values of F_2 (PMD) at the lowest $x = 0.015$ and Q^2 bin were up to 20% higher than both the NMC data and the predictions of the light-flavor MRSR2 PDFs. (see figure 2 (b)). About half of the difference originates from having used a leading order model for ΔxF_3 versus using our new measurement. The other half originates from having used the leading order slow rescaling corrections, instead of using a NLO massive charm production model, and from improved modeling of the low Q^2 PDFs (which changes the radiative corrections and the overall absolute normalization to the total neutrino cross sections).

In conclusion, the F_2 (PMI) values measured in neutrino-iron and muon-deuterium scattering show good agreement with the predictions of Next to Leading Order PDFs (using massive charm production schemes), thus resolving the long-standing discrepancy between the two sets of data. The first measurements of ΔxF_3 are higher than current theoretical predictions.

$d\sigma^2/Edx dy : 150 \text{ GeV}$

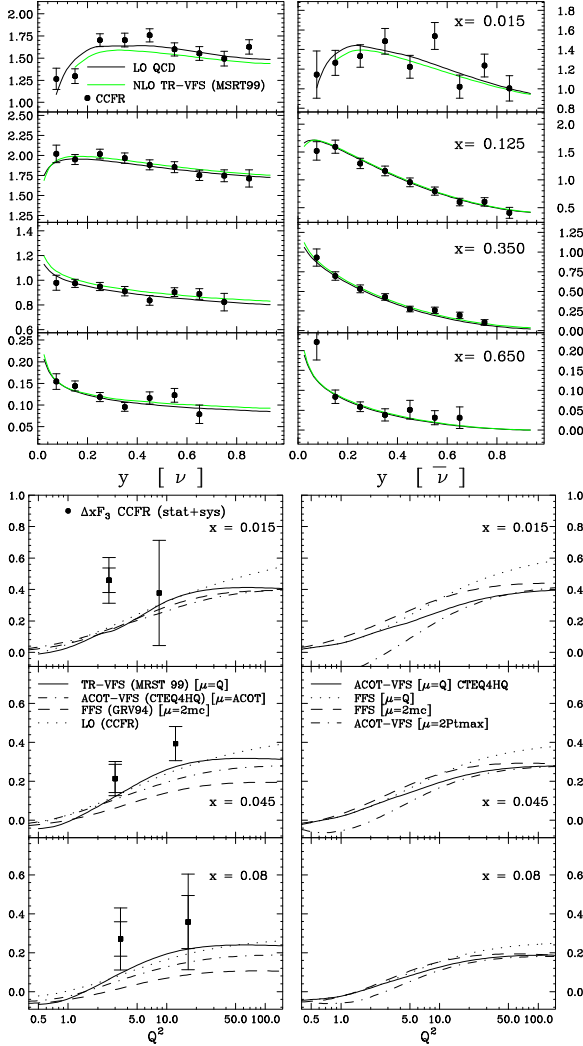


FIGURE 1. (a) Typical raw differential cross sections at $E_\nu = 150 \text{ GeV}$ (both statistical and systematic errors are included). (b) $\Delta x F_3$ data as a function of x compared with various schemes for massive charm production: RT-VFS(MRST), ACOT-VFS(CTEQ4HQ), FFS(GRV94), and LO(CCFR), a leading order model with a slow rescaling correction (left); Also shown is the sensitivity of the theoretical calculations to the choice of scale (right).

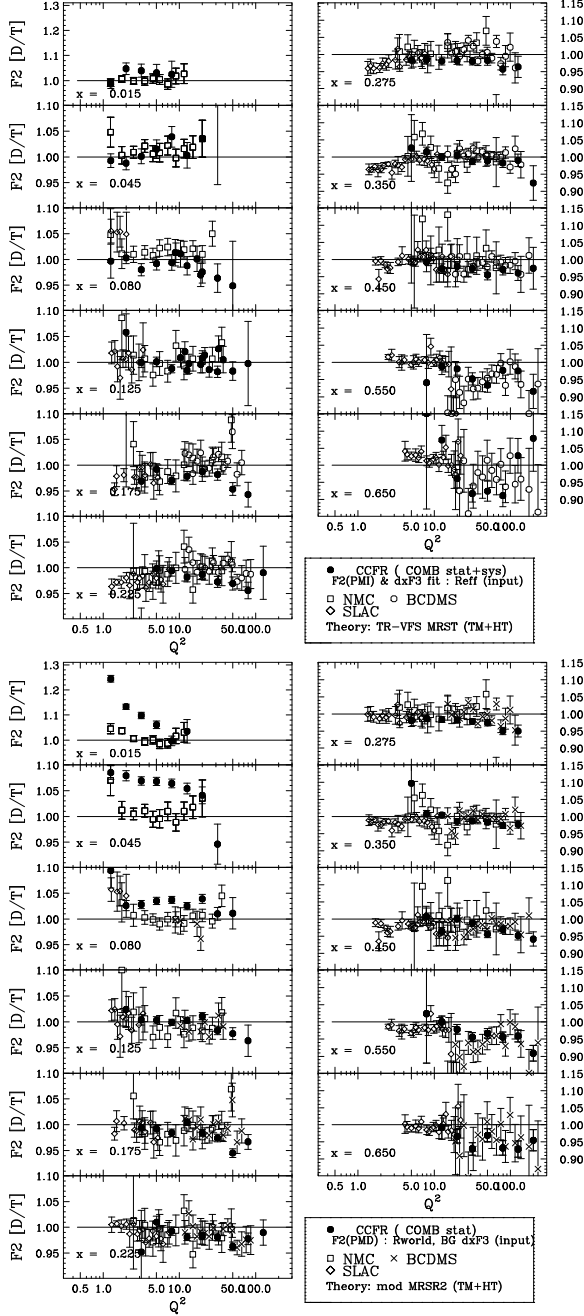


FIGURE 2. (a) Left side: The ratio (data/theory) of the F_2' (PMI) data divided by the predictions of TR-VFS(MRST) (with target mass and higher twist corrections). Both statistical and systematic errors are included. Also shown are the ratios of the F_2^{μ} (NMC) and F_2^e (SLAC) to the TR-VFS(MRST) predictions. (b) Right side: The ratio (data/theory) of the previous F_2' (PMD) data (and also F_2^{μ} (NMC) and F_2^e (SLAC)) divided by the predictions of the MRSR2 light-flavor PDFs (with target mass and higher twist corrections).